Heliyon 10 (2024) e28825

Contents lists available at ScienceDirect

Heliyon

journal homepage: www.cell.com/heliyon

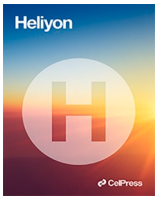

Research article

# The maternal-fetal neurodevelopmental groundings of preterm birth risk

Cesare Miglioli [c], Matteo Canini [a], Edoardo Vignotto [c], Nicolò Pecco [a], Mirko Pozzoni [b], Maria-Pia Victoria-Feser [c], Stéphane Guerrier [c,d], Massimo Candiani [b], Andrea Falini [a], Cristina Baldoli [a], Paolo I. Cavoretto [b,*], Pasquale A. Della Rosa [a]

[a] *Department of Neuroradiology, IRCCS San Raffaele Scientific Institute, Via Olgettina 60, Milan, 20132, Italy*
[b] *Department of Obstetrics and Gynecology, IRCCS San Raffaele Scientific Institute, Via Olgettina 60 Milan, 20132, Italy*
[c] *Research Center for Statistics, University of Geneva, Boulevard Du Pont-d'Arve 40, 1205 Geneva, Switzerland*
[d] *Faculty of Science, University of Geneva, Quai Ernest-Ansermet 30, 1211 Geneva, Switzerland*

ARTICLE INFO

*Keywords:*
Preterm birth
Preterm birth risk
Fetal neurodevelopment
fMRI
Fetal brain functional connectivity
Machine learning

ABSTRACT

*Background:* Altered neurodevelopment is a major clinical sequela of Preterm Birth (PTB) being currently unexplored in-utero.
*Aims:* To study the link between fetal brain functional (FbF) connectivity and preterm birth, using resting-state functional magnetic resonance imaging (rs-fMRI).
*Study design:* Prospective single-centre cohort study.
*Subjects:* A sample of 31 singleton pregnancies at 28–34 weeks assigned to a low PTB risk (LR) (n = 19) or high PTB risk (HR) (n = 12) group based on a) the Maternal Frailty Inventory (MaFra) for PTB risk; b) a case-specific PTB risk gradient.
*Methods:* Fetal brain rs-fMRI was performed on 1.5T MRI scanner. First, directed causal relations representing fetal brain functional connectivity measurements were estimated using the Greedy Equivalence Search (GES) algorithm. HR vs. LR group differences were then tested with a novel ad-hoc developed Monte Carlo permutation test. Second, a *MaFra-only* random forest (RF) was compared against a *MaFra-Neuro* RF, trained by including also the most important fetal brain functional connections. Third, correlation and regression analyses were performed between *MaFra-Neuro* class probabilities and i) the GA at birth; ii) PTB risk gradient, iii) perinatal clinical conditions and iv) PTB below 37 weeks.
*Results:* First, fewer fetal brain functional connections were evident in the HR group. Second, the *MaFra-Neuro* RF improved PTB risk prediction. Third, *MaFra-Neuro* class probabilities showed a significant association with: i) GA at birth; ii) PTB risk gradient, iii) perinatal clinical conditions and iv) PTB below 37 weeks.
*Conclusion:* Fetal brain functional connectivity is a novel promising predictor of PTB, linked to maternal risk profiles, ahead of birth, and clinical markers of neurodevelopmental risk, at birth, thus potentially "connecting" different PTB phenotypes.

* Corresponding author.
*E-mail addresses:* cesare.miglioli@unige.ch (C. Miglioli), canini.matteo@hsr.it (M. Canini), edoardovignotto@gmail.com (E. Vignotto), pecco.nicolo@hsr.it (N. Pecco), pozzoni.mirko@hsr.it (M. Pozzoni), maria-pia.victoriafeser@unige.ch (M.-P. Victoria-Feser), stephane.guerrier@unige.ch (S. Guerrier), candiani.massimo@hsr.it (M. Candiani), falini.andrea@hsr.it (A. Falini), baldoli.cristina@hsr.it (C. Baldoli), cavoretto.paolo@hsr.it (P.I. Cavoretto), dellarosa.pasquale@hsr.it (P.A. Della Rosa).

https://doi.org/10.1016/j.heliyon.2024.e28825
Received 9 October 2023; Received in revised form 25 March 2024; Accepted 26 March 2024
Available online 27 March 2024

## 1. Introduction

Preterm birth (PTB) (<37 weeks' gestational age (GA)) [1] is associated with increased risk of long-term neurodevelopmental outcomes [2–4]. Etiopathogenesis of PTB is multifactorial and takes the form of gestational constellations of both intrauterine (IU) and extrauterine (EU) factors quantifying the patient-specific risk for PTB [5]. However, during pregnancy, the reduction of PTB risk to a binary clinical outcome in terms of a GA birth cut-off disregards the effects of maternal frailties on the settlement of neurodevelopmental foundations during the fetal period.

Emerging fetal subcortico-cortical functional synchronization provides the means for the development and training of a nuclear set of cognitive tools during gestation progressively shaping a foundational cognitive development blueprint [6], geared towards leaving permanent brain-behavior imprints in the extrauterine environment.

Thus, PTB risk should not be limited to a gestational age cut-off at birth, however should be observed through the lens of maternal frailties, identified through the most informative IU-EU gestational constellations, and fetal neurodevelopment, characterized through the functional maturation of brain areas and networks, relevant for behavior and cognition during postnatal life.

The aim of the present study is to ground the degree of PTB risk in the gestational binding between an individualized maternal frailty profile and fetal subcortico-cortical connectivity imprints, extending PTB risk interventional projections beyond delivery, towards a neurodevelopmental time-continuum spanning from birth to infancy.

Namely, our goals were i) to trace brain connectivity between-group differences for fetuses classified at highrisk (HR) and lowrisk (LR) of PTB based upon a multidimensional assessment and characterization of maternal risk profiles; ii) to identify a candidate set of fetal brain functional (FbF) connections able to significantly contribute to the classification of PTB multidimensional maternal risk profiles and iii) to verify if viable PTB risk-responsive connections are significantly associated to the GA at birth, maternal category membership based on risk characterization, clinical markers of neurodevelopmental risk at birth, and can significantly explain PTB occurrence (below or above 37th gestational week (GW) at birth).

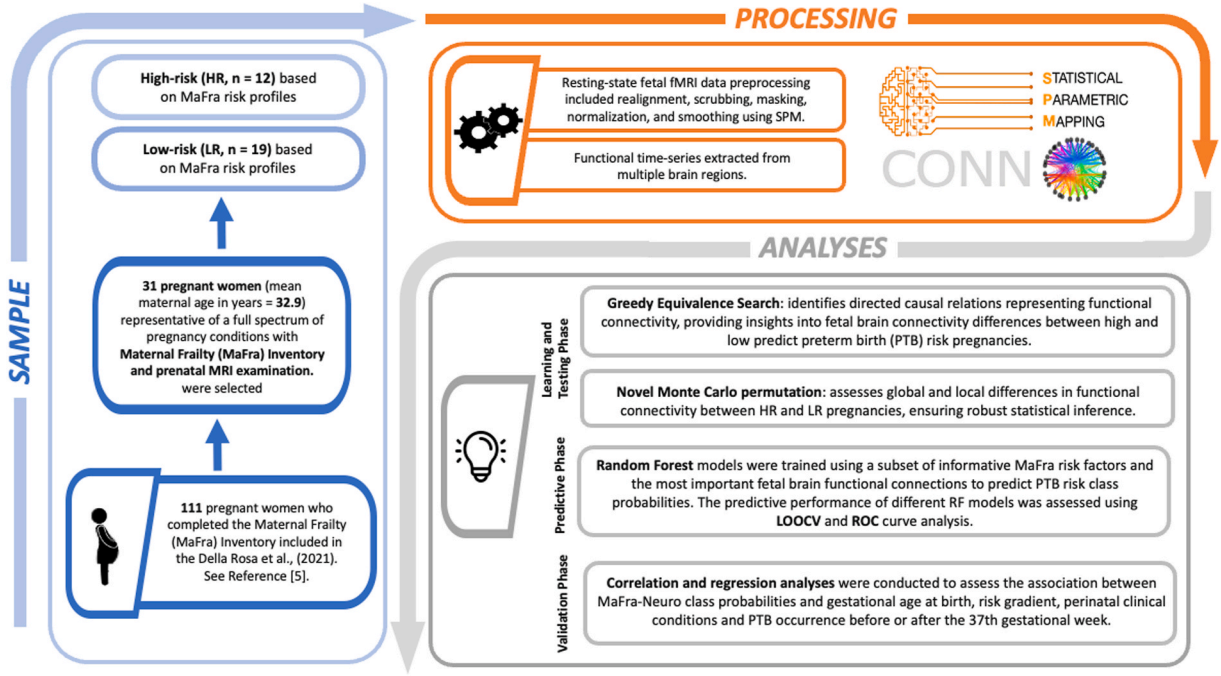


**Fig. 1. Flowchart of Study Design and Analysis Methods.** This figure outlines our comprehensive approach, starting with the selection of the study sample, through to data processing, and concluding with various analytical phases. Initially, from a group of 111 pregnant women, 31 were chosen based on a wide spectrum of pregnancy conditions as per the Maternal Frailty (MaFra) Inventory, with high-risk (HR) and low-risk (LR) groups categorized according to MaFra risk profiles. The processing phase involved meticulous preprocessing of resting-state fetal functional MRI data, including realignment and normalization, to extract functional time series from multiple brain regions. We then applied advanced statistical methods, such as Greedy Equivalence Search, Novel Monte Carlo permutation, and Random Forest (RF) models, to discern differences in brain connectivity between HR and LR pregnancies and to predict preterm birth (PTB) risk. Finally, correlation and regression analyses were employed to associate the predictive model outcomes, denoted as MaFra-Neuro class probabilities, with clinical outcomes such as gestational age at birth, risk gradient, perinatal clinical conditions and PTB occurrences.

## 2. Material and Methods

### 2.1. Participants

The sample was selected based on 111 pregnant women who completed the Maternal Frailty (MaFra) Inventory enrolled in the Della Rosa et al. (2021) study [5], within the Operative Unit of Gynecology and Obstetrics, at San Raffaele Hospital in Milan, Italy.

31 participants (mean maternal age in years = 32.9; StDev = 6.4; range = 18:44) were sampled from this pool of 111 pregnant women and assigned to a HR (n = 12) or LR (n = 19) group based on their MaFra intrauterine and/or extrauterine risk profiles [5] for inclusion in the FbF MRI protocol (see Fig. 1).

The sample of pregnant women (n = 31) encompassed a group of individuals with heterogeneous risks of PTB leading to an average increased risk of PTB for the whole group, due to the extensive presence of risk factors including short cervical length, pPROM, medically assisted procreation, prior PTB, pregnancy induced hypertention (PIH), placenta previa, preeclampsia, fetal growth restriction, complex autoimmune disease.

The study protocol was approved *a priori* by the Ethics Committee of the San Raffaele Hospital (EC Register of Opinions Number: 51/INT/2018). All pregnant women provided written and verbal informed consent for both MaFra administration and prenatal MRI examination. The study was conducted according to the principles of the Declaration of Helsinki. All imaging data were anonymized before further analysis. STROBE guidelines for reporting observational studies were followed [7].

#### 2.1.1. Participants – obstetric clinical assessment

All pregnancies underwent regular and standardized clinical assessment from the first trimester to birth, according to the local protocol with particular interest to tailoring intensity of follow-up and care according to the individual patient risk-profile. The data were collected from all pregnant women before the Coronavirus 19 pandemic outbreak, between June 2018 and Februrary 2020.

Each pregnant woman included in the study sample received a detailed clinical interview including the assessment of the MaFra Inventory [5]. All sampled participants underwent the first-trimester combined screening test at 11+0–13 + 6 weeks according to the Fetal Medicine Foundation United Kingdom guidelines (FMF-UK; www.fetalmedicine.org), which included: i) estimation of gestational age based upon the crown rump length measurement; ii) screening for chromosomal defects based upon fetal nuchal translucency, additional ultrasound markers and maternal serum concentrations of free β-human chorionic gonadotropin, pregnancy associated plasma protein-A and placental growth factor; iii) screening for preeclampsia based upon uterine arteries pulsatility index, mean arterial pressure and placental biomarkers cited above. The exclusion criteria were: fetuses with prenatal diagnosis of major malformation with subsequent medical abortion, twin pregnancies, pregnant women who did not sign the informed consent [5]. Low-dose Aspirin (150 mg) was recommended to all those with risk of preterm preeclampsia exceeding 1:150 according to the FMF-UK algorithm. Second trimester ultrasound was carried out in all cases at 19–21 weeks for anatomical survey, uterine arteries Doppler studies and cervical length measurement [8]. Cervical length was performed in all cases with an empty bladder and drawing a straight line with caliper between internal and external or across the endocervical mucosa; three repeated measurements were collected over 3 min of which the shortest was chosen for records. Vaginal natural progesterone 200 mg was administered to all pregnant women with cervical length below 20 mm and additional cervical cerclage was proposed to all pregnant women with ultrasound cervical length ≤10 mm. When amniotic sludge was diagnosed by ultrasound, according to the criteria described by Kusanovic et al., 2007 [9], additional antibiotics treatment was recommended as well as before cerclages, regardless of amniotic sludge or when clinically indicated based upon symptoms or microbiological cultures. Third trimester ultrasound was carried out between 26 and 36 weeks according to clinical indications (once at 32–36 weeks in low-risk pregnancies or repeatedly in high-risk cases according to clinical

**Table 1**
**P-value ordering of the fetal brain functional connections.** FbF edges (i.e. directional connections) with a more consistent presence either in the HR or in the LR group ordered by the p-value (smaller or equal to 0.10) obtained from a local (i.e. at edge level) permutation test. In italics the FbF edges present in at least 20% of subjects (7/31). The number of subjects with active connections in each group and the mean difference in GA at birth (active vs non active) are also reported.

| FbF Directional Connections | Edge p-value | Active Connections HR | Active Connections LR | Mean difference in GA at birth |
|---|---|---|---|---|
| *Brainstem → R Cortical Plate* | 0.008 | 0 | 8 | 1.61 |
| R Hippocampus → R Cerebellum | 0.014 | 4 | 0 | −2.57 |
| *R Subthalamic → R Lentiform* | 0.019 | 0 | 7 | 1.36 |
| *R Lentiform → R Hippocampus* | 0.019 | 0 | 7 | 1.25 |
| R Cortical Plate → R Cerebellum | 0.021 | 5 | 1 | −0.35 |
| L Lentiform → L Hippocampus | 0.037 | 0 | 6 | 0.7 |
| *L Caudate → L Cortical Plate* | 0.042 | 7 | 4 | −0.56 |
| *Brainstem → R Cerebellum* | 0.045 | 3 | 12 | 1.91 |
| *R Hippocampus → R Lentiform* | 0.059 | 5 | 2 | −3.27 |
| L Hippocampus → R Amygdala | 0.064 | 4 | 1 | −4.41 |
| L Cerebellum → R Amygdala | 0.068 | 0 | 5 | 1.17 |
| L Lentiform → R Subthalamic | 0.069 | 0 | 5 | 1.98 |
| R Cerebellum → R Cortical Plate | 0.071 | 0 | 5 | 1.05 |
| R Cortical Plate → L Cerebellum | 0.072 | 0 | 5 | 2.27 |
| *R Cortical Plate → R Lentiform* | 0.082 | 7 | 5 | −0.27 |

indications provided by individual physicians managing the cases). All pregnancies were also seen every 4–6 weeks according to their risk profile. Low-risk (LR) patients received an average of 6 screening clinical assessment (including visits and ultrasound scans), and high-risk (HR) patients were seen more often, particularly in the third trimester, with serial evaluations according to their risk profile and clinical needs. In each medical examination, cervical length, hematological and serological works, blood pressure measurement, weight and well-being assessment were investigated. Patients with progressive cervical shortening or significant other risks of iatrogenic or spontaneous prematurity or presenting with threatened preterm labor were hospitalized and treated accordingly based upon global clinical evaluation (course of betamethasone for fetal lung maturation, tocolysis with atosiban, antibiotics). All HR patients underwent a case-by-case clinical assessment and when the risk of PTB within 7 days was deemed high, a course of steroids with bethametasone 12 mg per day for 2 days was indicated. All patients received standardized intrapartum care with continuous cardiotocography in labour, and neonatal assessment and care provided by on call neonatologists.

#### *2.1.2. Participants – PTB risk characterization*

PTB risk and gradient characterization, based upon evaluation of risk factors with their specific magnitude, was performed by a senior obstetrician specialized in maternal-fetal medicine (PC), following the ACOG 2012 clinical management guidelines [10] and through the Maternal Frailty inventory of risk factors (MaFra) (see Ref. [5] for a full list of all included factors).

PTB risk was characterized through the evaluation of both IU and EU risk factors related to 1) obstetrical and gynecological history; 2) lifestyle before and during pregnancy (see Table 1 in Ref. [5] for maternal risk characterization and descriptives) and results of the first and second trimester clinical assessment following obstetric clinical assessment.

The PTB risk characterization gradient was instead defined by the qualitative evaluation of risk factors with their specific magnitude. Each risk factor was weighed with a qualitative approach and assessed as a whole over the total of factors present in each specific case, as defined in our previous study [5]. A 4-point Likert scale was used to characterize PTB risk in each participant on an incremental scale (i.e. 1- very low; 2- low, 3- high, 4- very high).

### *2.2. Fetal brain MRI data acquisition*

All the pregnant women included in the study sample underwent fetal MRI acquisition at the Pediatric Unit in the Department of Neuroradiology of the San Raffaele Hospital in Milan, Italy.

Fetal functional and structural MR scanning was performed on a Philips Achieva 1.5 T scanner (GW at fetal scan mean = 31.6; StDev = 1.92; median = 31.7; range = 27.6:34.7), using a 16 channels body coil supervised by an expert pediatric neuroradiologist (CB).

Fetal functional scans (rs-fMRI) consisted of GE EPI scans (TR = 2000 ms, TE = 30 ms, acquisition voxel size 2.81 × 2.86 × 3 mm, # slices = 25, slice gap = 0). Each rs-fMRI scan consisted of 60 vol lasting 2 sec each, for a total scanning time of 2 min per scan. Four-to-six consecutive rs-fMRI sessions (i.e. 240-360 scans, covering 8–12 min of continuous brain activity at rest were acquired for each fetus [11]. All pregnant women were asked not to eat within 3 h previous fetal MR scanning.

Fetal structural scans for clinical evaluation consisted of a T2 Single Shot Turbo Spin Echo scan on the axial, sagittal and coronal planes of the fetus, TR = 8000 ms, TE = 125 ms, voxel size 1.17 x 2.76 × 3 mm, #slices = 25, for a total scanning duration time of 17 sec. All fetuses showed no sign of fetal neurodevelopmental abnormality nor brain parenchymal signal alterations acknowledged by a specialized experienced neuroradiologist (CB) using structural MRI investigation.

### *2.3. Resting-state fetal fMRI data preprocessing*

Resting State functional volumes were preprocessed using a baseline fetal rs-fMRI preprocessing pipeline [12] in Statistical Parametric Mapping (SPM) (SPM12, University College London, available at http://www.fil.ion.ucl.ac.uk/spm/). The baseline fetal rs-fMRI preprocessing pipeline included the following steps: i) manual spatial reorientation in correct SPM orientation and origin set; ii) with-in session realignment to a session-specific reference image; iii) 1st pass with-in session scrubbing procedure including frame-to-mean (https://www.nitrc.org/projects/artifact_detect) and frame-to-frame estimates of motion and calculation of signal intensity changes [13,14]; iv) visual inspection and exclusion of with-in session outlier volumes; v) with-in session specific reference image masking to exclude maternal abdominal tissue; vi) realignment and calculation of the between-session mean reference masked image from with-in session-specific reference masked images; vii) 1st between-session realignment of all functional volumes to the between-session mean reference masked image; viii) 2nd pass between-session scrubbing procedure and between-session outlier volume exclusion; ix) 2nd between-session realignment post-scrubbing; x) between-session mean reference abdominal skull- and body-stripping using a subject-specific brain segmentation procedure a) for creation of an inner fetal brain mask based on subject-specific GW fetal tissue class probability maps [15] and b) for calculation of the deformation parameters for spatial normalization to fetal subject-specific GW standard space; xi) fetal inner-brain masking, spatial normalization and smoothing with a 4 mm gaussian kernel of all functional volumes.

### *2.4. Functional time series data Extraction*

The smoothed normalized rs-fMRI time series for all subjects underwent denoising procedures in the CONN functional connectivity toolbox (Version 18b) (CONN18b, available at https://web.conn-toolbox.org/) [16]. CONN's denoising step allows to identify potential inter-subject confounding effects (i.e. physiological noise, scanner magnetization) to the estimated BOLD signal through linear

regression. An anatomical component-based noise correction procedure (aCompCor) removes potential noise from the cerebrospinal and white matter regions of the brain at each voxel for each subject and session. BOLD signal components above 0.09Hz and below 0.008Hz are further removed with a temporal band-pass filtering procedure to minimize the influence of physiological noise. Following removal of potential confounding effects to the BOLD signal, the denoised mean BOLD parameters were computed considering all the voxels included in fetal brain regions of interest (ROIs) across the rs-fMRI time series for all subjects. Namely, the mean denoised BOLD time series parameters were extracted from the following fetal brain ROIs: left (L) and right (R) Thalamus, L and R Hippocampus, L and R Caudate Nucleus, L and R Amygdala, L and R Lentiform Nucleus (Globus Pallidus + Putamen) and L and R Subthalamic Nucleus, L and R Cerebellum, L and R Cortical Plate and Brainstem. Fetal brain ROI masks were defined using a subject-specific GW fetal brain parcellation [15] in the same standard fetal GW space of subject-specific normalized functional volumes.

### 2.5. Statistical Analysis

The statistical analyses conducted in this study are organized into three sequential phases: initially, the *learning and testing phase*; subsequently, the *predictive phase*; and finally, the *validation phase*.

In the first phase, the functional connectivity (FC) brain network of each subject was estimated. Networks of FbF connections were then used as inputs for a Monte Carlo permutation test, assessing evidence for fewer FbF connections in HR versus LR pregnancies. In the second phase, we compared the predictive performance of a *MaFra-only* random forest [17] (RF) classifier, trained solely with "degree of risk" factors representative of the MaFra [5], with a *MaFra-Neuro* RF, trained also with the inclusion of the most important FbF connections. In the third phase, correlation and regression analyses were performed between *MaFra-Neuro* class probabilities, obtained from the *MaFra-Neuro* RF classifier, and i) the GA at birth; ii) PTB risk gradient, iii) PTB below 37 weeks, iv) perinatal vital systems impairment' (pVSI) composite estimates and v) neonate size-at-birth classification scores.

In the following paragraphs, we provide a detailed description of the statistical procedures carried out in each distinct phase. All statistical analyses were conducted using R (version 3.6.0) [18]. The package *CompareCausalNetworks* was used to estimate the FC networks while the package *caret* for training the RF models. Statistical tests were performed at significance level 5% unless otherwise stated.

#### 2.5.1. Learning and testing phase

We define a generic brain network $N = (V, E)$ with nodes set $V = \{1, .., m\}$ and edges set $E \subseteq V \times V$. In our study, each node $j \in V$ represents a brain Region of Interest (ROI), and the edge set $E$ captures the dependency relationships among the ROIs. To learn these relationships, we need to impose a probabilistic graphical model [19] where V is associated with random variables $X_1, \ldots, X_m$ ($m = 17$ in our study). If causal relationships among the variables are of interest, we can specify a directed graphical model in which a directed edge j → k represents a causal effect of $X_j$ on $X_k$. Within this class of models, the most relevant is the Bayesian network [20]. In practice, under this modeling assumption, the presence/absence and the direction of an edge is inferred from observations (i.e., rs-fMRI time series) on each node $j \in V$. Learning these directed networks from observational data is known to be challenging [21] but it allows a researcher to conclude, for example, that brain Region A causally influences brain Region B which is one of the main end goals of FC analysis [21]. Following these considerations, we have chosen a causal search procedure i.e., the Greedy Equivalence Search (GES) algorithm [22], to learn the connectivity networks, as other well-known methods (e.g., the graphical lasso [23]) target only the presence/absence of an edge and not its direction. GES adds, removes, or inverts the direction of FbF connections between different ROIs until capturing maximal goodness-of-fit measured by the Bayesian Information Criterion (BIC) [24]. In the Supplementary Material, we provide a detailed review of the different methods that learn connectivity networks from fMRI data, and several motivations for the specific choice of GES among them. In addition, many studies have used GES with fMRI data [21] e.g., to investigate Autism spectrum disorder [25] or traumatic brain injury [26]. In our work, we have used GES on the single-subject preprocessed functional TS (n.tot. subjects = 31) (mean number of timepoints = 157; SD = 5.7; IQR = 44) to estimate the set of directed causal relations [21,27] that represent the FC of that specific subject (each FC matrix: 17x17 seeds = 289 FbF connections).

The FC networks learned by GES, were used as inputs to test, with a left-tailed specification, the research hypothesis of fewer FbF connections in HR versus LR pregnancies. First, we encoded the information on the edge set $E$ in an adjacency matrix $A$ for each subject in the sample. Within our context, the adjacency matrix is a (0, 1) matrix where a value of 1 for a given element $a_{jk}$ of $A$ with $j, k \in V$, indicates the presence of an edge (directed) from j to k. Conversely a value of 0 implies the absence of that same edge. As previously outlined, the adjacency matrix of each subject (i.e., a mathematical representation of its FC network) was estimated by GES on the preprocessed functional time series. Next, we aggregated information at subject level by counting how many connections were "active" (i.e., $a_{jk} = 1$) in the adjacency matrix of each subject. We stored these counts in a vector $\boldsymbol{c}$ with i-th component:

$$c_i = \sum_{j=1}^{m} \sum_{k=1}^{m} a_{jki}$$

Where $i \in \{1, \ldots, n\}$ denotes the specific subject considered in a sample of size $n$. In our study, $n = 31$ and the number of nodes $m = 17$. Moreover, if we name $G_1$ the group of HR pregnancies ($n_{G_1} = 12$) and $G_2$ the LR group ($n_{G_2} = 19$), we can express the observed average number of "active" connections in a generic group $G$ as:

$$\overline{c_G} = \frac{\sum_{i \in G} c_i}{n_G}$$

Where $n_G$ is the group size. At this point, we defined the test statistic $T$ which measures the discrepancy between the data and the null hypothesis $H_0$. Under the null, the population means (i.e., the average number of "active" FbF connections) of the two groups are equal and, given that we wanted evidence of fewer FbF connections in HR pregnancies versus LR (i.e., a left tailed test), we have chosen as test statistic the difference of the sample means of the two groups:

$$T = \overline{c_{G_1}} - \overline{c_{G_2}}$$

Large negative values of $T$ are evidence against $H_0$ because the average counts of "active" connections (i.e., present edges) would be then generally higher in $G_2$ with respect to $G_1$. To perform this test, the distribution of the test statistic $T$ under $H_{0\text{ should be specified}}$. We built the distribution by calculating all possible values of the test statistic under all possible rearrangements (i.e., permutations) of the observed components of the vector $\boldsymbol{c}$ in two groups of size $n_{G_1}$ and $n_{G_2}$. In our specific case, calculating all possible permutations would have been computationally unfeasible and thus we relied on the Monte Carlo method to obtain an approximate p-value with a standard procedure (see e.g. Ref. [28], ch.4). Thus, we developed a novel Monte Carlo permutation test that evaluates global differences in FC under all possible rearrangements (i.e., permutations) of the whole sample of subjects in two groups of size 12 (HR) and 19 (LR). We decided to perform 20000 permutations for any Monte Carlo permutation test presented in our study. This enabled us to have a very accurate estimate of the exact p-value however, in general, a value of 1000 is already considered safe in many contexts [28,29]. In addition, robustness checks on the permutation test were performed to avoid the influence of potential confounding factors such as difference in group sample sizes, unequal variances in the two groups, suboptimal inference on the direction of the FbF connections and different rs-fMRI time-series lengths. Indeed, taking inspiration from [30], the current testing procedure can be made robust to differences in group sample sizes (i.e., $n_{G_1} \neq n_{G_2}$) and potential *between-group* differences in the variances of the observed counts via *studentization*. This implies dividing the test statistic $T$ by an estimator of the standard deviation that corrects for both instances. Moreover, we considered as alternative test inputs also the undirected networks learned by GES for each single individual, since some evidence exists (e.g. [31]) that GES may not be optimal for estimating the direction of causal relationships but accurate in identifying when a connection is present. Furthermore, we explored the possibility of setting an equal length *within-group* to the rs-fMRI time series that we have observed on each node $j \in V$. Indeed, the original time series had different lengths (mean number of timepoints = 157; SD = 5.7; IQR = 44) and, since GES exploits them to infer the presence/absence (and the direction) of a given edge, this difference could have impacted the variability of the estimation procedure. In the Supplementary Material, we have also discussed other interesting alternative modifications of the proposed testing procedure and its place within the broader statistical literature. Finally, we applied the same permutation test locally (i.e., for each individual FbF connection), now with a two-tailed specification, to rank the importance of the directional connections through the p-values of the local tests. For example, to provide evidence for the FbF connection $j \to k$, with $j, k \in V$, being less present in group $G_1$ with respect to $G_2$, we defined a local test statistic $T_{jk} = \bar{a}_{jk}^{G1} - \bar{a}_{jk}^{G2}$ where $\bar{a}_{jk}^{G}$ represents the proportion of "active" $j \to k$ connections in a generic group $G$. Given this local specification, we then approximated the exact p-value once more with a MC permutation approach. This analysis helped us to both isolate the most important FbF connections, whose differences in proportions *between-groups* are either supporting or opposing the global test result, and drastically reduce the space of brain features (i.e., FbF connections) used in the following *predictive phase*.

### 2.5.2. Predictive phase

Initially, we obtained the out-of-sample classification errors, estimated by means of leave-one-out cross validation (LOOCV), of two distinct RF classifiers. The first one, was trained solely with a subset of the most informative "degree of risk" factors (n = 4/9), representative of the MaFra and present in at least 20% of the pregnant women in our sample (7/31) (i.e., antibiotics; cervical length; physical exercise in pregnancy; maternal anxiety). We named this RF model *MaFra-only* because it does not exploit any knowledge of the FC networks of the subjects. The second RF classifier was trained adding the most important FbF connections (Table 1), present in at least 20% of the subjects (7/31), to the subset of MaFra most informative risk factors. Thus, we named this RF model *MaFra-Neuro* as it combines standard "degree of risk" factors with FbF connectivity. PTB-risk class probabilities of the two RF classifiers were then obtained and we compared their predictive performance with a receiver operating characteristics (ROC) curve analysis to find the RF model with the best area under the curve (AUC).

### 2.5.3. Validation phase

We first considered the class probabilities of the *MaFra-Neuro* RF model, trained in the *predictive phase,* as a continuous measure that combines degree of maternal risk and FbF connectivity. This specific RF classifier includes both MaFra most informative risk factors and the most relevant FbF connections. *MaFra-Neuro* RF model class probabilities were reviewed for clinical plausibility, by an expert in maternal fetal medicine (P.C.), for each subject.

In addition, data from the clinical records of the newborns, following delivery of the pregnant women included in the study sample at the San Raffaele hospital (26 out of 31), was used to compute neonate size-at-birth classification scores (i.e. small, adequate or large for gestational age), based on the Intergrowth 21st birth weight centiles standards [32] and 'perinatal vital systems impairment' (pVSI) composite estimates. The pVSI scores captures variability related to the neonate's vital systems conditions, during the perinatal period, following delivery and before discharge.

To this end, for each vital system, we evaluated the presence or absence (i.e. dichotomous scoring) of a particular clinical condition

or medical procedure (so that the higher the number of clinical conditions and medical procedures, the higher the degree of impairment). Specifically, the respiratory system was characterized in terms of presence or absence of respiratory distress, conventional ventilation procedures, and mechanical ventilation procedures; the digestive system was characterized in terms of presence or absence of parenteral nutrition; the cardiocirculatory system was characterized in terms of presence or absence of arterial hypotension and Botallo's duct; the hematopoietic system was characterized in terms of presence or absence of anemy; the endocrine system was characterized in terms of presence or absence of hypoglycemia, and icterus.

A global estimate of vital systems impairment was then calculated as the average of dichotomous scores (i.e. presence or absence) for all conditions and procedures received by each neonate for each classified vital system. The total number of received pharmacological treatments was also calculated, as a further indicator of vital systems impairment. Namely, administration of surfactant, corticosteroids, inotropes, eritropoietin and opioid drugs were scored dichotomously. The pVSI score was then calculated by weighting (i.e. multiplying) the global vital system impairment estimate by the average number of pharmacological treatments received by each subject.

We then performed correlation and regression analyses to assess a) the association between *MaFra-Neuro* class probabilities and i) the GA at birth with a left-tailed Pearson product-moment correlation test; ii) the risk gradient, based on a qualitative evaluation of specific risk factors on an ordinal scale (i.e., 1- very low; 2- low, 3- high, 4- very high), with a right-tailed Spearman's rank correlation test; iii) the perinatal vital systems impairment' (pVSI) composite estimates with a right-tailed Spearman's rank correlation test; iv) the neonate size-at-birth classification scores with a left-tailed Spearman's rank correlation test b) the relationship between *MaFra-Neuro* class probabilities and birth occurring before or after the 37th GW coded as a binary variable, with a multivariate logistic regression controlling for the GW at scan.

## 3. Results

### 3.1. Learning and testing phase

The permutation test ($p = 0.0199$; n.perm. $= 20000$) revealed fewer FbF connections in HR versus LR pregnancies. Our robustness checks on some potential confounding factors (see *Learning and Testing Phase* in the Material and Methods section) confirmed the above result. Indeed, the original test specification corrections addressed at: a) allowing for differences in group sample sizes or unequal variances in the two groups via *studentization* ($p = 0.0133$; n.perm. $= 20000$), b) preventing a suboptimal inference on the direction of the FbF connections by focusing only on undirected FbF connections ($p = 0.0316$; n.perm. $= 20000$) and c) avoiding an additional

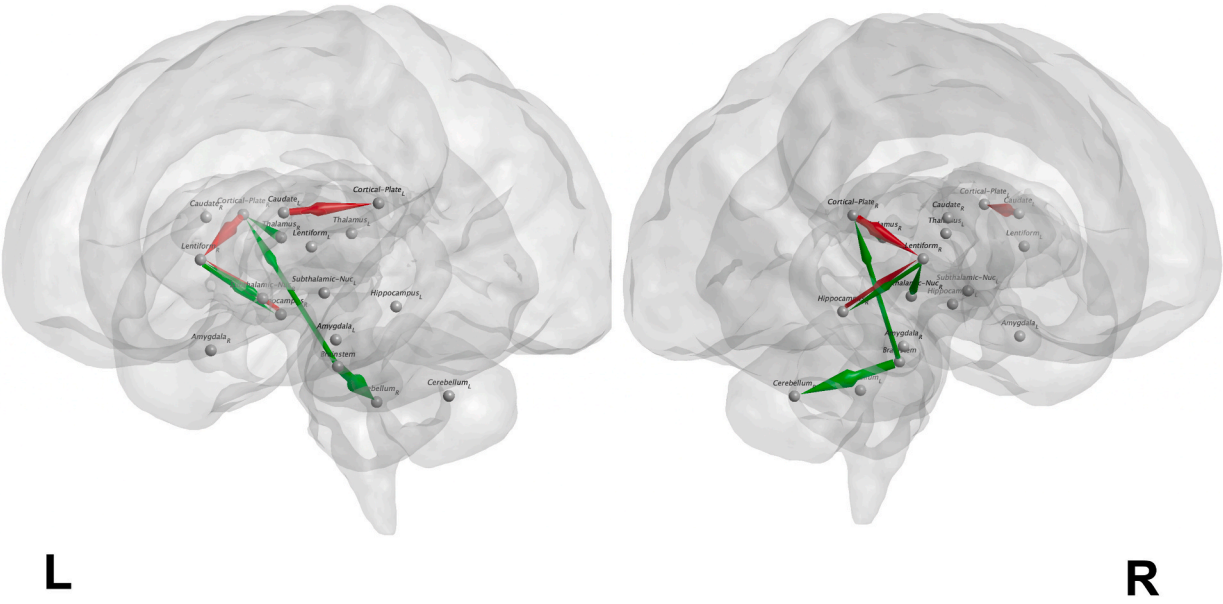


**Fig. 2. Visualization of Significant Fetal Brain Functional Connections in Prediction Analysis.** This figure presents brain network renderings using the BrainNet Viewer [50], showcasing significant directional connections (fetal brain functional -FbF- edges) identified during the predictive phase of our study. These edges, determined as statistically significant with $p < 0.1$ (refer to Table 1), are observed in a minimum of 20% of participants (7 out of 31 subjects). The visualizations are depicted from both left and right sagittal orientations, illustrating the integration of FbF edges with the most informative markers of "degree of risk" (MaFra factors). Color coding is employed to differentiate the prevalence of these edges: green for those consistent in the low-risk (LR) group and red for the high-risk (HR) group, providing a clear visual representation of the directional connections differentiating the two groups. (For interpretation of the references to colour in this figure legend, the reader is referred to the Web version of this article.)

variability in the GES estimation procedure by setting an equal length within-group to the rs-fMRI time series ($p = 0.0145$; n.perm. = 20000), validated the conclusion of the original permutation test. Main positive/negative drivers either supporting or opposing the global test result are provided in Table 1, ordered by local p-values ($p < 0.1$), together with the number of active connections per group and mean difference in GA at birth between subjects with active versus subjects with inactive connections. A higher presence of active connections in the HR (LR) group is associated to a negative (positive) mean difference in GA. Among the most important (i.e., $p < 0.1$) FbF connections, the ones present in at least 20% of the subjects (7/31) are: L caudate to L cortical plate, R hippocampus to R lentiform nucleus, R cortical plate to R lentiform nucleus which were more active in the HR group (see Fig. 2). On the other hand, brainstem to R cortical plate, R subthalamic nucleus to R lentiform nucleus, R lentiform nucleus to R hippocampus, brainstem to R cerebellum connections were more consistently active in the LR group (see Fig. 2).

### 3.2. Predictive phase

In the LOOCV analysis, the *MaFra-only* RF classifier achieved a best accuracy of 74.19% (i.e., a classification error of 25.81%) and an AUC of 0.7039. On the other hand, the *MaFra-Neuro* RF classifier yielded a best accuracy of 83.87% (i.e., a classification error of 16.13%) and an AUC of 0.8684. We also present the graphs of the two ROC curves (Fig. 3) and the variable importance ranking (Table 2) of the RF *MaFra-Neuro* classifier.

### 3.3. Validation phase

The 31 newborns were classified as preterm-born (<37 weeks' GA) (n = 6) or at term-born (>37 weeks' GA) (n = 25), based on gestational age at delivery collected for the entire study sample of pregnant women (mean weeks' GA at delivery = 38,4, StDev = 2,78, min-max range = 29,3–41,4).

No signs of broncopulmonary displasia, retinopathy of prematurity and auditory impairment, cerebral infarction, hemorrhage, and encephalopathy of prematurity were evident in all screened neonates (n = 26).

Correlation analyses showed a significant association between *MaFra-Neuro* class probabilities and i) the GA at birth (Pearson correlation $r = -0.43$; $p = 0.008$; CI = −1.00: 0.14), ii) the PTB risk gradient characterization (Spearman's rank correlation rho = 0.46; $p = 0.005$; CI = 0.12:0.70), iii) the 'perinatal vital systems impairment' (pVSI) composite estimates (Spearman's rank correlation rho = 0.44; $p = 0.012$; CI = 0.07:0.71), iv) the neonate size-at-birth classification scores (Spearman's rank correlation rho = −0.41; $p = 0.019$; CI = −0.69: 0.03). The multivariate logistic regression model having birth occurring before or after the 37th GW as a dependent variable and *MaFra-Neuro* class probabilities as the independent variable, controlling for GW at scan, showed a significant explanatory effect (z-value = 2.07; $p = 0.038$, CI = 1.25:14.38). A detailed output of the model is presented in Table 3.

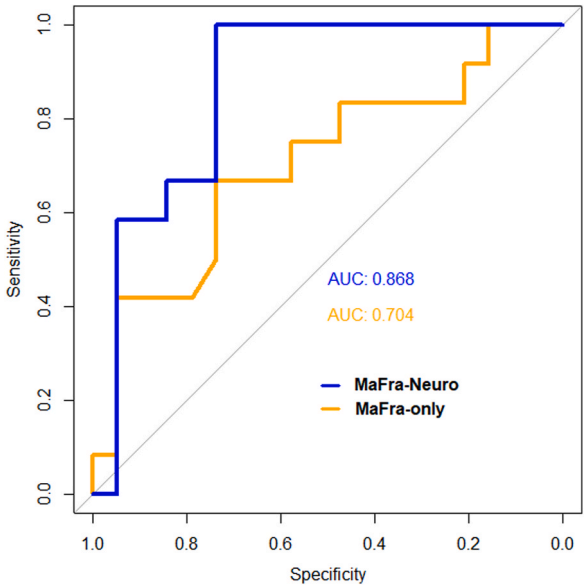


**Fig. 3. Visual Comparison of Model Predictive Efficacy Using ROC Analysis.** This figure illustrates the comparative effectiveness of two predictive models using Receiver Operating Characteristic (ROC) curves and Area Under the Curve (AUC) metrics. The first model, denoted as *'MaFra-Neuro'*, incorporates both the most informative maternal 'degree of risk' (MaFra) factors and the most consistently observed fetal brain functional (FbF) directional connections. The second model, termed *'MaFra-only'*, includes only the subset of the most informative MaFra 'degree of risk' factors. The ROC curves demonstrate the true positive rate versus the false positive rate of each model, while the AUC provides a quantitative measure of the model's ability to correctly classify subjects into the correct risk category.

**Table 2**
**Variable importance ranking of the Random Forest model that combines degree of maternal risk and brain connectivity.** Mean leave one out (LOO) variable importance ranking for the RF classifier trained with both the subset of MaFra "degree of risk" factors and the most consistently present FbF directional connections (see Table 1).

| Predictive Variables | Mean LOO Variable Importance |
|---|---|
| Cervical Length | 100 |
| Brainstem → R Cortical Plate | 59.82 |
| L Caudate → L Cortical Plate | 58.58 |
| R Cortical Plate → R Lentiform Nucleus | 46.95 |
| Brainstem → R Cerebellum | 36.37 |
| R Subthalamic Nucleus → R Lentiform Nucleus | 35.46 |
| R Lentiform Nucleus → R Hippocampus | 33.60 |
| R Hippocampus → R Lentiform Nucleus | 30.10 |
| Anxiety | 14.80 |
| Physical Exercise | 2.70 |
| Antibiotics Medication | 0.32 |

## 4. Discussion

This study showed that altered neurodevelopment with differential or excessive fetal brain connectivity is not a mere consequence of PTB, instead it anticipates birth, being demonstrated in-utero. More so, in-utero fetal brain connectivity showed specific neurodevelopmental signatures and a significant relationship to PTB. A combined model based upon maternal frailties and fetal neurodevelopment significantly predicted PTB.

### *4.1. Neurobiological groundings*

During the third trimester of pregnancy, the functional synchronization of subcortical and cortical activity of neuronal pools into coherent information processing networks is a core neurobiological feature of the fetal brain maturation process [33–35]. Particularly, networks underlying goal-directed behavioral interactions with the environment develop with high ontogenetic priority and appear in 'prototypical', adult-like configurations already at fetal functional investigations performed during the third trimester [6,36]. Consistently, our results revealed that functional signatures for both groups were found in terms of subcortical connectivity patterns related to purposed behavior functionality (i.e. cerebellum, brainstem, hippocampus and striatum). However, despite this general pattern of shared functional maturation, important differences emerged between groups.

First, striato-cortical synchronization emerged as an exclusive functional signature of the HR group. The establishment and consolidation of connectivity in the cortical plate is an important index of maturation of brain functionality and, under normal circumstances, this process is ontogenetically scheduled to take place throughout the third trimester of pregnancy [37,38]. To this end, our results could suggest that in a physiological context characterized by a heightened risk of PTB, maturation of connectivity pathways essential for perinatal behavioral adaptation could be triggered and prioritized [36,39]. In fact, the striatum relays inputs through parallel loops in the cortico-striato-thalamo-cortical circuit [40] and 'functionally coaches' connectivity of sensorimotor, frontal and limbic cortices respectively for sensorimotor integration, motor and cognitive control regulation, emotion and reward modulation [41,42].

Second, the LR group brainstem-cerebellum edge, which plays a pivotal role for the development of gross and fine motor function [43], and the involvement of the subthalamic nucleus in subcortical circuitry were highlighted as exclusive features of the LR group. This latter structure is a major convergence site for processing of information related to motor function, decision making and attribution of emotional valence [44–46]. Thus, its absence from edges characterizing the HR group could suggest that early striato-cortical synchronization could come at the cost of later processing complexity and information integration.

Third, a lentiform-hippocampus edge was observed for both groups, although with inverse directionality (i.e. lentiform to hippocampus for LR and vice-versa). Effective striatal-hippocampal connectivity underlies encoding facilitation for unexpected familiar stimuli, a key component for the regulation of exploratory behaviors [47]. In adults, hippocampal overactivation within this circuitry is associated with aberrant salience/valence attribution, which in turn is a key hallmark of several psychopathological conditions [48–50]. Considering the higher susceptibility of preterm borns to develop psychiatric disorders (including ADHD, schizophrenia,

**Table 3**
**Multivariate logistic regression model output.** Birth occurring before or after the 37th GW (i.e. PTB) is the dependent variable while MaFra-Neuro, i.e. the continuous measure that combines degree of maternal risk and FbF connectivity, and the GW at scan are the independent variable.

| Dependent Variable: PTB (<37 GW) | Number of observations: 31 | | | |
|---|---|---|---|---|
| Predictors | **Estimate (SE)** | **CI 95%** | **Z-value** | **P-value** |
| (Intercept) | 12.78 (10.48) | (-6.66, 36.89) | 1.22 | 0.222 |
| MaFra Neuro | 6.53 (3.15) | (1.25, 14.38) | 2.07 | 0.038 |
| GW at scan | −0.57 (0.36) | (-1.44, 0.06) | −1.59 | 0.113 |

anxiety and depression) [51,52] our findings could suggest that maternal and fetal conditions heightening the risk for prematurity could also lead to alterations of the functional balance between regions pivotal for the emergence of the brain-behavior tie, thus driving a grounding, detrimental impact on its long-term developmental trajectory [53].

Neuronal migration and synaptogenesis are paramount in determining subcortical-cortical functional organization. From the developmental pathoconnectomics perspective [36], many clinical [5,10] and environmental [5] PTB risk factors occurring before conception and during pregnancy may induce considerable developmental perturbations of the functional brain connectome. Despite the causes of PTB are deeply grounded in maternal, fetal or placental risk factors, poor fetal brain connectomic evidence exists for identifying possible crossroads between neurodevelopmental disruptions and the emergence of a subcortical-cortical functional homeostasis in advance of PTB.

Namely, in this context, alterations in neurodevelopment due to a PTB risk-sensitive prenatal functional "miswiring" [54,55] may change brain-behaviour receptiveness and adaptation to postnatal environmental conditions (i.e. differential susceptibility [56]) resulting in specific combinations of PTB risk-sensitive neurofunctional phenotypes.

Della Rosa et al. [5] have already shown in a previous study that preterm birth risk estimation can be achieved by means of a hierarchical procedure selecting intrauterine and extrauterine factors through a cost-effective model including a limited group of predictors. In this study, the addition of PTB risk-sensitive connections to the aforementioned model, including only maternal risk factors, improved model performance for the classification of maternal PTB risk. In addition, the subject-wise presence/absence of PTB risk-sensitive connections resulted significantly associated to PTB risk gradient characterization, GA at birth, perinatal vital systems impairment evaluation, size-at-birth classification and significantly predicted PTB outcome.

Perinatal medical conditions and birthweight are two well-known factors associated to neurodevelopmental outcomes during infancy and childhood, both in conjunction and independently of premature delivery [57,58].

Moving from our hypothesis, and from the pathoconnectomics perspective [36], fetal brain functional connectivity can be thus framed as a potential biomarker, not only able to predict preterm birth outcome, ahead of birth, in interaction with the maternal environment, but also related to neonatal clinical indicators of potential aberrant neurodevelopmental patterns, following premature birth, thus enhancing its relevance to prenatal care and intervention strategies.

### 4.2. Clinical groundings

This study opens room to a cutting-edge vision of PTB, in which neurodevelopmental perturbations already begin in utero. Since potential aberrant neurodevelopment has classically been traced back to preterm birth outcome, our results push the search of the noxae of aberrant neurodevelopment already in utero and before birth, in the prenatal rather than postnatal life.

It is true that PTB produces postnatal consequences on neurodevelopment due to organ immaturity potentially leading to complications related to abnormal neurodevelopment (e.g., brain hypoxia due to abnormal lung function, parenchimal haemorrage, nutritional perturbations due to bowel disease of prematurity, etc). However, it is also true that in-utero conditions affect neurodevelopment before birth, adding on insults and noxae to premature birth itself. Our results are in line with two decades of research on PTB phenotypes [59,60], with profiles traced back to unknown reasons showing better postnatal neurodevelopment as compared to those led back to infection or fetal anomaly [60,61].

However, future research should encompass larger sample sizes for a finer-grained delineation of PTB risk-sensitive neurofunctional phenotypes and for exploration of potential interactions effects between risk factors, which may play different roles when present alone or acting in combination.

Lastly, if aberrant neurodevelopment is already demonstrated in utero and not due to PTB, the question raises concerning clinical benefit of PTB prevention aimed at prolonging pregnancy in all cases at risk. Theoretically, future in-utero intervention studies may define the selection of cases in which postponing birth may provide the greatest clinical benefit vs. those in which this approach may be less beneficial or further deteriorate neurodevelopment, based upon multifactorial etiological phenotyping, as described by recent major research on PTB phenotyping [59–63].

### 4.3. Conclusions

This study supports the groundings of PTB phenotyping, proposed recently by the INTERBIO-21st study, which identified 8 major phenotypes: no main condition detected, infections, preeclampsia, fetal distress, intrauterine growth restriction, severe maternal disease, bleeding and congenital anomaly [61].

Thus, these results encourage future prediction studies with larger samples based upon fetal brain connectomics as a novel promising risk marker for redefining preterm birth also in neurodevelopmental terms and aimed at PTB phenotyping through a common denominator linking spontaneous or iatrogenic PTB (and related risk factors) to abnormal neurodevelopment. On this basis, the route towards studies aimed at prevention of aberrant neurodevelopment with individualized early preventive strategies may be initiated, in order to improve fetal and neonatal outcome. This approach will stimulate prospective intervention studies assessing whether aberrant neurodevelopmental trajectories may possibly be rerouted already in utero along with PTB prevention and geared towards implementing precision medicine approaches addressed at individual patient-specific treatment for PTB.

## Ethics approval statement

This study was conducted in full accordance with ethical principles, including the World Medical Association Declaration of

Helsinki. The research protocol was reviewed and approved by the Ethics Committee of the San Raffaele Hospital under EC Register of Opinions Number: 51/INT/2018.

## Patient consent statement

All pregnant women provided written and verbal informed consent for both MaFra administration and prenatal MRI examination.

## Funding

This work was supported by the Italian Ministry of Health's "Ricerca Finalizzata 2016" (grant number RF-2016-02364081; Principal Investigator: Dr. Pasquale Anthony Della Rosa).

## Data availability statement

The code developed for this study to perform the statistical tests and referred to throughout the Statistical Analysis section and Supplementary Material of the paper is publicly available at the following repository: https://github.com/CaesarXVII/Fetal_brain_connectivity_and_preterm_birth_risk. Anonymized data that supports the findings of this study will be made available upon reasonable request from P.A.D.R (dellarosa.pasquale@hsr.it). and in accordance with the Ethics Committee of the San Raffaele Hospital.

## CRediT authorship contribution statement

**Cesare Miglioli:** Writing – review & editing, Writing – original draft, Visualization, Validation, Software, Methodology, Formal analysis, Data curation, Conceptualization. **Matteo Canini:** Writing – original draft, Investigation, Data curation, Conceptualization. **Edoardo Vignotto:** Writing – review & editing, Software, Methodology, Formal analysis, Conceptualization. **Nicolò Pecco:** Writing – review & editing, Visualization, Software, Formal analysis. **Mirko Pozzoni:** Writing – review & editing, Investigation, Data curation. **Maria-Pia Victoria-Feser:** Writing – review & editing, Supervision, Methodology, Formal analysis. **Stéphane Guerrier:** Writing – review & editing, Supervision, Methodology, Formal analysis. **Massimo Candiani:** Writing – review & editing, Supervision, Resources, Project administration, Investigation, Funding acquisition. **Andrea Falini:** Writing – review & editing, Supervision, Resources, Project administration, Investigation. **Cristina Baldoli:** Writing – review & editing, Supervision, Resources, Project administration, Investigation, Funding acquisition. **Paolo I. Cavoretto:** Writing – review & editing, Writing – original draft, Supervision, Project administration, Investigation, Conceptualization. **Pasquale A. Della Rosa:** Writing – review & editing, Writing – original draft, Supervision, Project administration, Methodology, Investigation, Funding acquisition, Formal analysis, Data curation, Conceptualization.

## Declaration of competing interest

The authors declare that they have no known competing financial interests or personal relationships that could have appeared to influence the work reported in this paper.

## Acknowledgments

The authors would also like to thank all the participants for their participation and their motivation.

## Supplementary Material

Supplementary data to this article can be found online at https://doi.org/10.1016/j.heliyon.2024.e28825.

## References

[1] H. Blencowe, S. Cousens, M.Z. Oestergaard, D. Chou, A.-B. Moller, R. Narwal, A. Adler, C.V. Garcia, S. Rohde, L. Say, J.E. Lawn, National, regional, and worldwide estimates of preterm birth rates in the year 2010 with time trends since 1990 for selected countries: a systematic analysis and implications, Lancet 379 (2012) 2162–2172, https://doi.org/10.1016/S0140-6736(12)60820-4.

[2] J.L. Cheong, L.W. Doyle, A.C. Burnett, K.J. Lee, J.M. Walsh, C.R. Potter, K. Treyvaud, D.K. Thompson, J.E. Olsen, P.J. Anderson, A.J. Spittle, Association between Moderate and late preterm birth and neurodevelopment and social-emotional development at age 2 years, JAMA Pediatr. 171 (2017) e164805, https://doi.org/10.1001/jamapediatrics.2016.4805.

[3] E.F. Bell, S.R. Hintz, N.I. Hansen, C.M. Bann, M.H. Wyckoff, S.B. DeMauro, M.C. Walsh, B.R. Vohr, B.J. Stoll, W.A. Carlo, K.P. Van Meurs, M.A. Rysavy, R. M. Patel, S.L. Merhar, P.J. Sánchez, A.R. Laptook, A.M. Hibbs, C.M. Cotten, C.T. D'Angio, S. Winter, J. Fuller, A. Das, Eunice kennedy shriver national Institute of child Health and human development neonatal research network, mortality, in-hospital morbidity, care practices, and 2-year outcomes for extremely preterm infants in the US, 2013-2018, JAMA 327 (2022) 248–263, https://doi.org/10.1001/jama.2021.23580.

[4] U. Kiechl-Kohlendorfer, E. Ralser, U.P. Peglow, G. Reiter, R. Trawöger, Adverse neurodevelopmental outcome in preterm infants: risk factor profiles for different gestational ages, Acta Paediatr. 98 (2009) 792–796, https://doi.org/10.1111/j.1651-2227.2009.01219.x.

[5] P.A. Della Rosa, C. Miglioli, M. Caglioni, F. Tiberio, K.H.H. Mosser, E. Vignotto, M. Canini, C. Baldoli, A. Falini, M. Candiani, P. Cavoretto, A hierarchical procedure to select intrauterine and extrauterine factors for methodological validation of preterm birth risk estimation, BMC Pregnancy Childbirth 21 (2021) 306, https://doi.org/10.1186/s12884-021-03654-3.

[6] M. Canini, P. Cavoretto, P. Scifo, M. Pozzoni, A. Petrini, A. Iadanza, S. Pontesilli, R. Scotti, M. Candiani, A. Falini, C. Baldoli, P.A. Della Rosa, Subcortico-cortical functional connectivity in the fetal brain: a cognitive development blueprint, Cereb. Cortex Commun 1 (2020) tgaa008, https://doi.org/10.1093/texcom/tgaa008.

[7] E. von Elm, D.G. Altman, M. Egger, S.J. Pocock, P.C. Gøtzsche, J.P. Vandenbroucke, The strengthening the reporting of observational studies in epidemiology (STROBE) statement: guidelines for reporting observational studies, Int. J. Surg. 12 (2014) 1495–1499, https://doi.org/10.1016/j.ijsu.2014.07.013.

[8] L.J. Salomon, C. Diaz-Garcia, J.P. Bernard, Y. Ville, Reference range for cervical length throughout pregnancy: non-parametric LMS-based model applied to a large sample, Ultrasound Obstet. Gynecol. 33 (2009) 459–464, https://doi.org/10.1002/uog.6332.

[9] J.P. Kusanovic, J. Espinoza, R. Romero, Clinical significance of the presence of amniotic fluid 'sludge' in asymptomatic patients at high risk for spontaneous preterm delivery, Ultrasound Obstet. Gynecol. 30 (2007) 706–714.

[10] American College of Obstetricians and Gynecologists, Committee on Practice Bulletins—Obstetrics, ACOG practice bulletin no. 127: management of preterm labor, Obstet. Gynecol. 119 (2012) 1308–1317, https://doi.org/10.1097/AOG.0b013e31825af2f0.

[11] K.R.A. Van Dijk, T. Hedden, A. Venkataraman, K.C. Evans, S.W. Lazar, R.L. Buckner, Intrinsic functional connectivity as a tool for human connectomics: theory, properties, and optimization, J. Neurophysiol. 103 (2010) 297–321, https://doi.org/10.1152/jn.00783.2009.

[12] N. Pecco, M. Canini, K.H.H. Mosser, M. Caglioni, P. Scifo, A. Castellano, P. Cavoretto, M. Candiani, C. Baldoli, A. Falini, P.A.D. Rosa, RS-FetMRI: a MATLAB-SPM based tool for pre-processing fetal resting-state fMRI data, Neuroinformatics 20 (2022) 1137–1154, https://doi.org/10.1007/s12021-022-09592-5.

[13] J.D. Power, K.A. Barnes, A.Z. Snyder, B.L. Schlaggar, S.E. Petersen, Spurious but systematic correlations in functional connectivity MRI networks arise from subject motion, Neuroimage 59 (2012) 2142–2154, https://doi.org/10.1016/j.neuroimage.2011.10.018.

[14] J.D. Power, A. Mitra, T.O. Laumann, A.Z. Snyder, B.L. Schlaggar, S.E. Petersen, Methods to detect, characterize, and remove motion artifact in resting state fMRI, Neuroimage 84 (2014) 320–341, https://doi.org/10.1016/j.neuroimage.2013.08.048.

[15] A. Gholipour, C.K. Rollins, C. Velasco-Annis, A. Ouaalam, A. Akhondi-Asl, O. Afacan, C.M. Ortinau, S. Clancy, C. Limperopoulos, E. Yang, J.A. Estroff, S. K. Warfield, A normative spatiotemporal MRI atlas of the fetal brain for automatic segmentation and analysis of early brain growth, Sci. Rep. 7 (2017) 476, https://doi.org/10.1038/s41598-017-00525-w.

[16] S. Whitfield-Gabrieli, A. Nieto-Castanon, Conn: a functional connectivity toolbox for correlated and anticorrelated brain networks, Brain Connect. 2 (2012) 125–141, https://doi.org/10.1089/brain.2012.0073.

[17] L. Breiman, Random forests, Mach. Learn. 45 (2001) 5–32, https://doi.org/10.1023/A:1010933404324.

[18] R.C. Team, R: A Language and Environment for Statistical Computing, R foundation for statistical computing, Vienna, 2021. No Title, https://cir.nii.ac.jp/crid/1370576118723163397. (Accessed 11 September 2023).

[19] S.L. Lauritzen, Graphical Models, vol. 17, Clarendon Press, 1996.

[20] P.J. Causality, Cambridge university press 2009, (n.d.).

[21] T. Henry, K. Gates, Causal search procedures for fMRI: review and suggestions, Behaviormetrika 44 (2017) 193–225, https://doi.org/10.1007/s41237-016-0010-8.

[22] D.M. Chickering, Optimal structure identification with greedy search, J. Mach. Learn. Res. 3 (2002) 507–554.

[23] J. Friedman, T. Hastie, R. Tibshirani, Sparse inverse covariance estimation with the graphical lasso, Biostatistics 9 (2008) 432–441.

[24] G. Schwarz, Estimating the dimension of a model, Ann. Stat. 6 (1978) 461–464.

[25] C. Hanson, S.J. Hanson, J. Ramsey, C. Glymour, Atypical effective connectivity of social brain networks in individuals with autism, Brain Connect. 3 (2013) 578–589.

[26] E. Dobryakova, O. Boukrina, G.R. Wylie, Investigation of information flow during a novel working memory task in individuals with traumatic brain injury, Brain Connect. 5 (2015) 433–441.

[27] C. Glymour, K. Zhang, P. Spirtes, Review of causal discovery methods based on graphical models, Front. Genet. 10 (2019). https://www.frontiersin.org/articles/10.3389/fgene.2019.00524. (Accessed 11 September 2023).

[28] A.C. Davison, D.V. Hinkley, Bootstrap Methods and Their Application, 1997.

[29] A. Gandy, Sequential implementation of Monte Carlo tests with uniformly bounded re sampling risk, J. Am. Stat. Assoc. 104 (2009) 1511.

[30] E. Chung, J.P. Romano, Exact and asymptotically robust permutation tests, Ann. Stat. 41 (2013) 484–507, https://doi.org/10.1214/13-AOS1090.

[31] J.A. Mumford, J.D. Ramsey, Bayesian networks for fMRI: a primer, Neuroimage 86 (2014) 573–582.

[32] J. Villar, L.C. Ismail, C.G. Victora, E.O. Ohuma, E. Bertino, D.G. Altman, A. Lambert, A.T. Papageorghiou, M. Carvalho, Y.A. Jaffer, M.G. Gravett, M. Purwar, I. O. Frederick, A.J. Noble, R. Pang, F.C. Barros, C. Chumlea, Z.A. Bhutta, S.H. Kennedy, International standards for newborn weight, length, and head circumference by gestational age and sex: the Newborn Cross-Sectional Study of the INTERGROWTH-21st Project, Lancet 384 (2014) 857–868, https://doi.org/10.1016/S0140-6736(14)60932-6.

[33] I. Kostović, N. Jovanov-Milošević, The development of cerebral connections during the first 20–45 weeks' gestation, Semin. Fetal Neonatal Med. 11 (2006) 415–422, https://doi.org/10.1016/j.siny.2006.07.001.

[34] H.-J. Park, K. Friston, Structural and functional brain networks: from connections to cognition, Science 342 (2013) 1238411, https://doi.org/10.1126/science.1238411.

[35] V. Menon, Developmental pathways to functional brain networks: emerging principles, Trends Cogn. Sci. 17 (2013) 627–640, https://doi.org/10.1016/j.tics.2013.09.015.

[36] A. Jakab, Developmental pathoconnectomics and advanced fetal MRI, Top. Magn. Reson. Imaging 28 (2019) 275, https://doi.org/10.1097/RMR.0000000000000220.

[37] I. Kostović, M. Judaš, The development of the subplate and thalamocortical connections in the human foetal brain, Acta Paediatr. 99 (2010) 1119–1127, https://doi.org/10.1111/j.1651-2227.2010.01811.x.

[38] Z. Molnár, H.J. Luhmann, P.O. Kanold, Transient cortical circuits match spontaneous and sensory-driven activity during development, Science 370 (2020) eabb2153, https://doi.org/10.1126/science.abb2153.

[39] M.E. Thomason, L.E. Grove, T.A. Lozon, A.M. Vila, Y. Ye, M.J. Nye, J.H. Manning, A. Pappas, E. Hernandez-Andrade, L. Yeo, S. Mody, S. Berman, S.S. Hassan, R. Romero, Age-related increases in long-range connectivity in fetal functional neural connectivity networks in utero, Dev. Cogn. Neurosci. 11 (2015) 96–104, https://doi.org/10.1016/j.dcn.2014.09.001.

[40] G.E. Alexander, M.R. DeLong, P.L. Strick, Parallel organization of functionally segregated circuits linking basal ganglia and cortex, Annu. Rev. Neurosci. 9 (1986) 357–381.

[41] S.N. Haber, B. Knutson, The reward circuit: linking primate anatomy and human imaging, Neuropsychopharmacology 35 (2010) 4–26, https://doi.org/10.1038/npp.2009.129.

[42] S.N. Haber, The place of dopamine in the cortico-basal ganglia circuit, Neuroscience 282 (2014) 248–257, https://doi.org/10.1016/j.neuroscience.2014.10.008.

[43] M. Manto, J.M. Bower, A.B. Conforto, J.M. Delgado-García, S.N.F. da Guarda, M. Gerwig, C. Habas, N. Hagura, R.B. Ivry, P. Mariën, M. Molinari, E. Naito, D. A. Nowak, N. Oulad Ben Taib, D. Pelisson, C.D. Tesche, C. Tilikete, D. Timmann, Consensus paper: roles of the cerebellum in motor control—the diversity of ideas on cerebellar involvement in movement, Cerebellum 11 (2012) 457–487, https://doi.org/10.1007/s12311-011-0331-9.

[44] J.G. McHaffie, T.R. Stanford, B.E. Stein, V. Coizet, P. Redgrave, Subcortical loops through the basal ganglia, Trends Neurosci. 28 (2005) 401–407, https://doi.org/10.1016/j.tins.2005.06.006.

[45] S. Marceglia, M. Fumagalli, A. Priori, What neurophysiological recordings tell us about cognitive and behavioral functions of the human subthalamic nucleus, Expert Rev. Neurother. 11 (2011) 139–149, https://doi.org/10.1586/ern.10.184.

[46] S.K.H. Tan, Y. Temel, A. Blokland, H.W.M. Steinbusch, V. Visser-Vandewalle, The subthalamic nucleus: from response selection to execution, J. Chem. Neuroanat. 31 (2006) 155–161, https://doi.org/10.1016/j.jchemneu.2006.01.001.
[47] A. Kafkas, D. Montaldi, Striatal and midbrain connectivity with the hippocampus selectively boosts memory for contextual novelty, Hippocampus 25 (2015) 1262–1273, https://doi.org/10.1002/hipo.22434.
[48] T. Winton-Brown, A. Schmidt, J.P. Roiser, O.D. Howes, A. Egerton, P. Fusar-Poli, N. Bunzeck, A.A. Grace, E. Duzel, S. Kapur, P. McGuire, Altered activation and connectivity in a hippocampal–basal ganglia–midbrain circuit during salience processing in subjects at ultra high risk for psychosis, Transl. Psychiatry 7 (2017), https://doi.org/10.1038/tp.2017.174 e1245–e1245.
[49] D.J. Lodge, A.A. Grace, Hippocampal dysregulation of dopamine system function and the pathophysiology of schizophrenia, Trends Pharmacol. Sci. 32 (2011) 507–513, https://doi.org/10.1016/j.tips.2011.05.001.
[50] D.J. Lodge, A.A. Grace, Developmental pathology, dopamine, stress and schizophrenia, Int. J. Dev. Neurosci. 29 (2011) 207–213, https://doi.org/10.1016/j.ijdevneu.2010.08.002.
[51] C. Arpino, E. Compagnone, M.L. Montanaro, D. Cacciatore, A. De Luca, A. Cerulli, S. Di Girolamo, P. Curatolo, Preterm birth and neurodevelopmental outcome: a review, Childs Nerv, Off. Syst. 26 (2010) 1139–1149, https://doi.org/10.1007/s00381-010-1125-y.
[52] A.T. Bhutta, M.A. Cleves, P.H. Casey, M.M. Cradock, K.J.S. Anand, Cognitive and behavioral outcomes of school-aged children who were born PretermA meta-analysis, JAMA 288 (2002) 728–737, https://doi.org/10.1001/jama.288.6.728.
[53] M. Canini, N. Pecco, M. Caglioni, A. Katušić, I.Ž. Išasegi, C. Oprandi, P. Scifo, M. Pozzoni, L. Lorioli, G. Garbetta, A. Poloniato, M.G.N. Sora, P.I. Cavoretto, G. Barera, M. Candiani, I. Kostović, A. Falini, C. Baldoli, P.A. Della Rosa, Maternal anxiety-driven modulation of fetal limbic connectivity designs a backbone linking neonatal brain functional topology to socio-emotional development in early childhood, J. Neurosci. Res. 101 (2023) 1484–1503, https://doi.org/10.1002/jnr.25207.
[54] L. Uddin, K. Supekar, V. Menon, Typical and atypical development of functional human brain networks: insights from resting-state fMRI, Front. Syst. Neurosci. 4 (2010). https://www.frontiersin.org/articles/10.3389/fnsys.2010.00021. (Accessed 11 September 2023).
[55] M. Rubinov, E. Bullmore, Fledgling pathoconnectomics of psychiatric disorders, Trends Cogn. Sci. 17 (2013) 641–647, https://doi.org/10.1016/j.tics.2013.10.007.
[56] J. Belsky, M.J. Bakermans-Kranenburg, M.H. van Ijzendoorn, For better and for worse: differential susceptibility to environmental influences, Curr. Dir. Psychol. Sci. 16 (2007) 300–304, https://doi.org/10.1111/j.1467-8721.2007.00525.x.
[57] I.S. Baron, K. Erickson, M.D. Ahronovich, R. Baker, F.R. Litman, Cognitive deficit in preschoolers born late-preterm, Early Hum. Dev. 87 (2011) 115–119, https://doi.org/10.1016/j.earlhumdev.2010.11.010.
[58] C.S.H. Aarnoudse-Moens, N. Weisglas-Kuperus, J.B. van Goudoever, J. Oosterlaan, Meta-analysis of neurobehavioral outcomes in very preterm and/or very low birth weight children, Pediatrics 124 (2009) 717–728, https://doi.org/10.1542/peds.2008-2816.
[59] J. Villar, A.T. Papageorghiou, H.E. Knight, M.G. Gravett, J. Iams, S.A. Waller, M. Kramer, J.F. Culhane, F.C. Barros, A. Conde-Agudelo, Z.A. Bhutta, R. L. Goldenberg, The preterm birth syndrome: a prototype phenotypic classification, Am. J. Obstet. Gynecol. 206 (2012) 119–123, https://doi.org/10.1016/j.ajog.2011.10.866.
[60] F.C. Barros, A.T. Papageorghiou, C.G. Victora, J.A. Noble, R. Pang, J. Iams, L. Cheikh Ismail, R.L. Goldenberg, A. Lambert, M.S. Kramer, M. Carvalho, A. Conde-Agudelo, Y.A. Jaffer, E. Bertino, M.G. Gravett, D.G. Altman, E.O. Ohuma, M. Purwar, I.O. Frederick, Z.A. Bhutta, S.H. Kennedy, J. Villar, For the international fetal and newborn growth consortium for the 21st century (INTERGROWTH-21st), the distribution of clinical phenotypes of preterm birth syndrome: implications for prevention, JAMA Pediatr. 169 (2015) 220–229, https://doi.org/10.1001/jamapediatrics.2014.3040.
[61] J. Villar, M.C. Restrepo-Méndez, R. McGready, F.C. Barros, C.G. Victora, S. Munim, A.T. Papageorghiou, R. Ochieng, R. Craik, H.C. Barsosio, J.A. Berkley, M. Carvalho, M. Fernandes, L. Cheikh Ismail, A. Lambert, S.A. Norris, E.O. Ohuma, A. Stein, C.O.O. Tshivuila-Matala, K.T. Zondervan, A. Winsey, F. Nosten, R. Uauy, Z.A. Bhutta, S.H. Kennedy, Association between preterm-birth phenotypes and differential morbidity, growth, and neurodevelopment at age 2 Years: results from the INTERBIO-21st newborn study, JAMA Pediatr. 175 (2021) 483–493, https://doi.org/10.1001/jamapediatrics.2020.6087.
[62] M.S. Kramer, A. Papageorghiou, J. Culhane, Z. Bhutta, R.L. Goldenberg, M. Gravett, J.D. Iams, A. Conde-Agudelo, S. Waller, F. Barros, H. Knight, J. Villar, Challenges in defining and classifying the preterm birth syndrome, Am. J. Obstet. Gynecol. 206 (2012) 108–112, https://doi.org/10.1016/j.ajog.2011.10.864.
[63] R.L. Goldenberg, M.G. Gravett, J. Iams, A.T. Papageorghiou, S.A. Waller, M. Kramer, J. Culhane, F. Barros, A. Conde-Agudelo, Z.A. Bhutta, H.E. Knight, J. Villar, The preterm birth syndrome: issues to consider in creating a classification system, Am. J. Obstet. Gynecol. 206 (2012) 113–118, https://doi.org/10.1016/j.ajog.2011.10.865.